Bull. Mater. Sci., Vol. 35, No. 5, October 2012, pp. 719–725. © Indian Academy of Sciences.

Photoluminescence quenching of semiconducting polymer nanoparticles in presence of Au nanoparticles

SANTANU BHATTACHARYYA and AMITAVA PATRA*
Department of Materials Science, Indian Association for the Cultivation of Science, Kolkata 700 032, India

MS received 17 February 2012

Abstract. **In this report, we have demonstrated the photoluminescence quenching and energy transfer properties of semiconducting polymer nanoparticles, poly (*N*-vinylcarbazole) (PVK) in presence of different sized Au nanoparticles by steady state and time-resolved spectroscopy. We have described the quenching phenomena by sphere of action static quenching mechanism and both dynamic and static quenching processes are found in these systems. PL quenching values are 24·22% and 57·3% for 14 nm and 18 nm Au nanoparticles, respectively. It is found that the radiative and nonradiative decay have been modified with the size of Au nanoparticles. PL quenching and shortening of decay time regarding polymer nanoparticles in presence of Au nanoparticles suggest the nonradiative energy transfer process. The values of energy transfer are 6·7%, 49·5% and 53·38% from PVK polymer nanoparticles to 3 nm, 14 nm and 18 nm Au nanoparticles, respectively. Using FRET and SET equations we have calculated the average distance of donor PVK polymer nanoparticles and acceptor Au nanoparticles.**

Keywords. **Photoluminescence quenching; semiconducting polymer nanoparticles; Au nanoparticles; time resolved spectroscopy.**

1. Introduction

Semiconducting conjugated polymeric nanoparticles are very much applicable for their multifunctional activities e.g. imagining, bio-sensing, drugs delivery, photonics and opto-electronics (Yu *et al* 1995; Kietze *et al* 2003; Wu *et al* 2008; Kim *et al* 2010). The super quenching and hyper-efficient energy transfer phenomena of water soluble conjugated polymer molecules attached with Au nanoparticles have been reported previously (Fan *et al* 2003). Kong *et al* (2007) reported various photophysical properties of PVK polymer nanoparticles doped by MEH–PPV. It was previously reported that the PL efficiency of Eu-complex varies with changing nature of the semiconducting polymer host (Chowdhury *et al* 2005). Interactions of different semiconducting polymer nanoparticles with Au nanoparticles have been demonstrated very recently (Bhattacharyya *et al* 2010). Application of polymer nanoparticles based fluorescence resonance energy transfer using nanoscopic environment is still in the embryonic stage. Further investigations in this field are necessary for an in-depth understanding of the phenomenon for developing new challenging photonic devices.

Dulkeith *et al* (2002) have shown the modification of radiative and nonradiative properties of lissamine dye in presence of chemically attached different sized Au nanoparticles. They have compared their experimental findings with theoretical results derived from Gerstan–Nitzan model. There are several reports on the photophysical properties and energy transfer phenomena of different semiconducting quantum dots and fluorophore in presence of different sized Au nanoparticles (Ghosh *et al* 2004; Cheng *et al* 2006; Soller *et al* 2007). In this report we have analysed the photoluminescence quenching mechanism of PVK polymer nanoparticles in presence of different sized (3 nm, 14 nm and 18 nm) Au nanoparticles. The quenching phenomena follows sphere of action static quenching model. According to this model certain fraction of PVK polymer nanoparticles are quenched due to static interaction with Au nanoparticles at their excited state. Rest of the fraction is quenched by collisional mechanism. Therefore, both static and dynamic quenching would be present in such a system. We would like to address a few issues: whether the size of Au nanoparticles influences on the quenching behaviour and on the modification of radiative and nonradiative rates of PVK polymer nanoparticles. Assuming modification of nonradiative decay to be responsible for the resonance energy transfer from PVK to Au nanoparticles, we have demonstrated size dependent variation of resonance energy transfer from PVK to different sized Au nanoparticles by time-resolved spectroscopic study. We have also calculated the distance between Au nanoparticles and PVK polymer nanoparticles by FRET and surface energy transfer mechanism.

2. Experimental

2.1 *Materials*

Chloroauric acid ($HAuCl_4 \cdot 3H_2O$) (Loba Chemie), trisodium citrate (Merck), PVK [poly (9-vinylcarbazole)] (Aldrich),

*Author for correspondence (msap@iacs.res.in)

MPA [3-mercaptopropanoic acid] (Aldrich), sodium hydroxide (Merck), sodium borohydride (Merck) and distilled tetrahydrofuran (Merck) were used in the present study without further purification.

2.2 *Experimental procedure*

PVK conducting polymer nanoparticles were prepared by typical reprecipitation method (Wu *et al* 2008; Bhattacharyya *et al* 2010). 1 mg/ml solution of PVK was prepared in distilled tetrahydrofuran. 200 μl of this THF solution was rapidly injected to 20 ml of distilled water under vigorous stirring. After 5–10 min of stirring, it was ultrasonicated for 30 min. Finally, we obtained aqueous suspensions of PVK polymer nanoparticles. Then THF was removed by vacuum evaporation followed by filtration through 0·2 micron filter. The suspensions became stable for 5–7 days.

To prepare smaller sized Au nanoparticles, the well known borohydride reduction method was used. Briefly, we added 500 μl MPA into 10 ml of distilled water. The aqueous solution turned to acidic. The pH of this solution became 3–4. 12 ml of this 0·5 M sodium hydroxide solutions was added to this MPA solutions. The resultant pH of this solution became 8. The concentration of MPA turned to 0·17 M. Then, 10 ml 0·1 mM aqueous solutions of $HAuCl_4$ and $3H_2O$ were taken. 100 μl of the previously prepared MPA solution was added to it. Next 0·3 ml 0·1 M ice cold $NaBH_4$ was dropwise added to it under vigorous stirring. After 10 min of stirring the solution became brown indicating the formation of small sized Au nanoparticles. A small amount of MPA capped 3 nm Au nanoparticles was added to 20 ml of distilled water to maintain Au nanoparticles concentration of $0{\cdot}1 \times 10^{-8}$ M. 200 μl THF solution of PVK was rapidly injected to this $0{\cdot}1 \times 10^{-8}$ M 3 nm Au nanoparticles solution under vigorous stirring followed by 30 min of ultrasonication. As a result we prepared PVK polymer nanoparticles suspension in 3 nm MPA capped Au colloidal suspensions.

To obtain larger sized Au nanoparticles, well known Frens method (Frens 1973) has been followed. In this method it is possible to control size of the particles by varying [Au (III)/citrate] ratio during the reduction process. Briefly, three different aqueous solutions of 47·5 ml $HAuCl_4$, $3H_2O$ (containing 0·01 g of gold solution) were heated to boiling. Then 2·5 ml of 2% and 1% sodium citrate solutions were added to the boiling solutions under vigorous stirring to get 14 nm and 18 nm Au nanoparticles, respectively. The colour of the first solution (2·5 ml 2% sodium citrate added) changes from light yellow to deep red through the appearance of bluish gray colour which persists for 5–10 min. For the second solution (2·5 ml 1% sodium citrate added) changes from light yellow to pinkish red through the appearance of this particular bluish gray colour. Then, each of these solutions was allowed to boil for another 20 min. Finally, these solutions were cooled down to room temperature under stirring condition. Thus, we obtained 14 nm deep red and 18 nm pinkish red solution of Au nanoparticles. Then appropriate amounts of each of these solutions were added to distilled water to maintain 20 ml $0{\cdot}1 \times 10^{-8}$ M Au nanoparticles in each case. Similarly 200 μl THF solution of PVK was rapidly injected to each of these solutions under vigorous stirring followed by ultrasonication. Similar vacuum evaporation and filtration through 0·2 micron filter was done. Finally, PVK nanoparticles suspensions in 14 nm and 18 nm Au colloidal solutions, respectively were obtained.

The transmission electron microscopy (TEM) images were taken using a JEOL–TEM 2010 transmission electron microscope with an operating voltage of 200 kV. Room temperature optical absorption spectra were obtained with an UV-vis spectrophotometer (shimadzu). The emission spectra of all the samples were recorded in a Fluoromax-P (HORIBA JOBIN YVON) luminescence spectrometer. For the time correlated single photon counting (TCSPC) measurement, samples were excited at 340 nm using a picosecond NANO-LED IBH 340. The following expression was used to analyse the experimental time resolved fluorescence decays, $P(t)$:

$$P(t) = b + \sum_{i}^{n} \alpha_i \exp\left(-\frac{t}{\tau_i}\right). \tag{1}$$

Here, n is the number of emissive species and b the baseline correction (d.c. offset), and α_i and τ_i are the pre-exponential factors and excited state fluorescence lifetimes associated with the ith component, respectively. The average life time, $\langle\tau\rangle$, was calculated from the following formula

$$\langle\tau\rangle = \sum_{i}^{n} \alpha_i \tau_i^2 \Big/ \sum_{i}^{n} \alpha_i \tau_i. \tag{2}$$

3. Results and discussion

3.1 *Morphological analysis*

Figure 1 depicts SEM image of pure PVK polymer nanoparticles. From SEM image it is clear that these polymer nanoparticles are nearly spherical having size distribution range of 60–80 nm. During injection of THF-solution of polymer into water (poor solvents for these kinds of polymer molecules) under stirring condition, the solution is divided into many droplets by strong shearing force. Simultaneously THF molecules quickly diffuse into water to make the polymer chains exposed to water and the polymer chains are coiled up to form polymer nanoparticles (Kong *et al* 2007). Figure 2 depicts TEM images of different sizes of Au nanoparticles and distribution of size in presence of PVK polymer nanoparticles.

3.2 *Steady state data and quenching mechanism*

Figure 3a shows normalized absorption spectra of different sized Au nanoparticles. Surface plasmon band is not observed for smaller particles (~3 nm) due to quantum confinement effect and strong dampening of plasmon oscillation. The surface plasmon bands are at 520 nm and 524 nm for

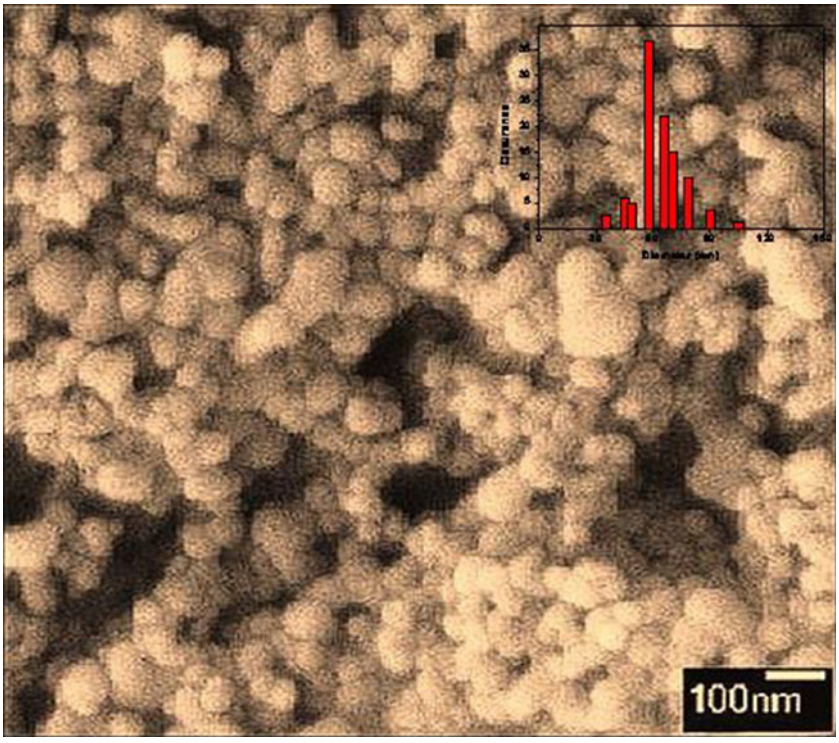

Figure 1. SEM image of PVK polymer nanoparticles.

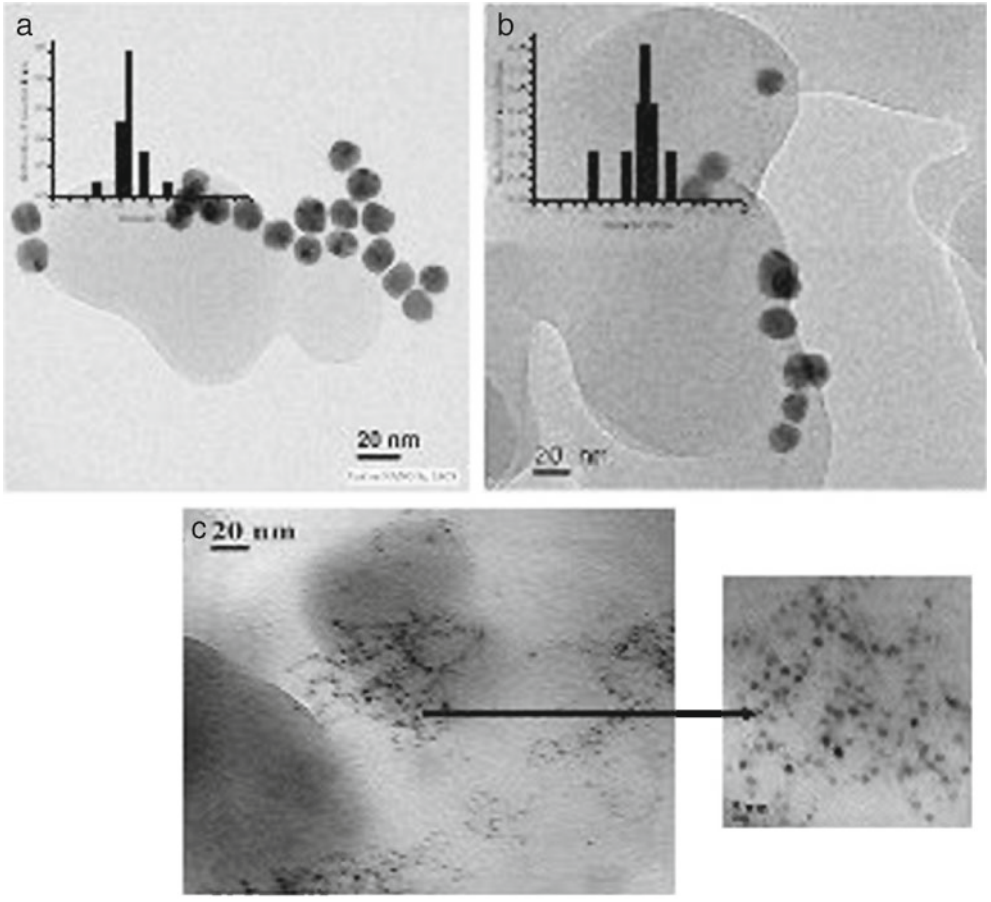

Figure 2. TEM images of PVK polymer nanoparticles in presence of **a**. 14 nm, **b**. 18 nm and **c**. 3 nm Au nanoparticles.

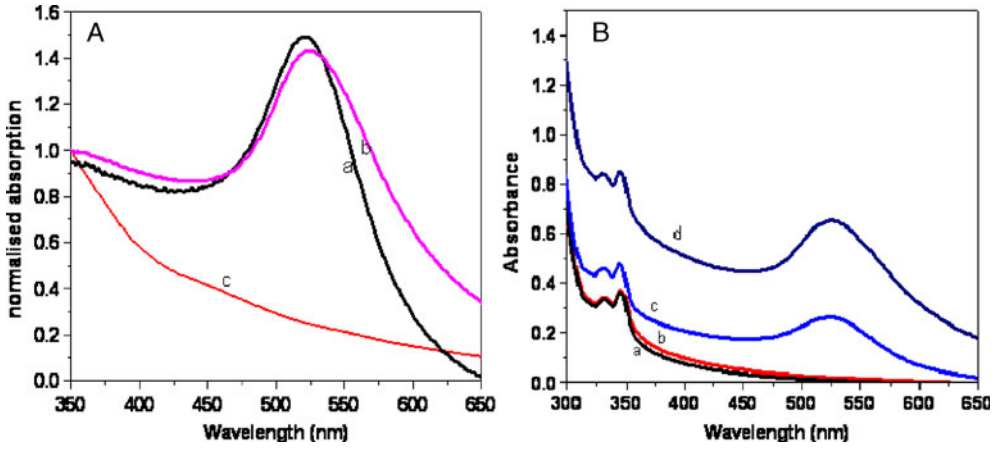

Figure 3. (**A**) Normalized UV-Vis spectra of a. 14 nm, b. 18 nm and c. 3 nm Au nanoparticles and (**B**) UV-Vis spectra of **a.** pure PVK, **b.** PVK+ 3 nm Au, **c.** PVK + 14 nm Au and **d**. PVK + 18 nm Au (particles concentration of Au is $0{\cdot}1 \times 10^{-8}$M in each case).

14 nm and 18 nm Au nanoparticles, respectively. The extinction coefficient of 3 nm particle is $0{\cdot}5 \times 10^6$ $M^{-1}cm^{-1}$. For 14 nm and 18 nm particles the extinction coefficients are $2{\cdot}11 \times 10^8$ $M^{-1}cm^{-1}$ and $6{\cdot}28 \times 10^8$ $M^{-1}cm^{-1}$ respectively. It matches well with the data described in previous literature (Link and El-Sayed 1999). Figure 3b shows absorption spectra of PVK in absence and presence of different sized Au nanoparticles. The peak position of PVK (almost at 340 nm) (Wu *et al* 2008; Bhattacharyya *et al* 2010) remains almost constant in presence of different sized Au nanoparticles. The molar extinction coefficient increases with increasing size of Au nanoparticles. The overlap between SPR band of Au nanoparticles and emission spectra of PVK polymer nanoparticles is very small and the overlap integral cannot be calculated in case of 3 nm Au nanoparticles. The overlap integrals are $4{\cdot}67 \times 10^{18}$ M^{-1} cm^{-1} nm^4 and $1{\cdot}56 \times 10^{19}$ M^{-1} cm^{-1} nm^4 for 14 nm and 18 nm Au nanoparticles, respectively. Figure 4 shows PL quenching spectra of PVK polymer nanoparticles in case of different sized Au nanoparticles. In case of 3 nm Au nanoparticles there is no quenching. There are 24·2% and 57·3% PL quenching for 14 nm and 18 nm Au nanoparticles, respectively. It is to be noted that the concentration of quencher Au nanoparticles remains constant ($0{\cdot}1 \times 10^{-8}$M) for each case. Thus, size of the quencher Au nanoparticles influences the photoluminescence quenching of PVK polymer nanoparticles. Figure 5a shows Stern–Volmer plot of pure PVK in presence of 14 nm and 18 nm Au nanoparticles. We observe a positive deviation of *S–V* plot in both the cases. The presence of static component in quenching is the cause of this type of positive deviation. The fractional intensity I_0/I is given by the product of both static and dynamic quenching. Therefore,

$$I_0/I = (1 + K_s[Q])(1 + K_{sv}[Q])$$
$$= 1 + K_1[Q] + K_2[Q]^2, \quad (3)$$

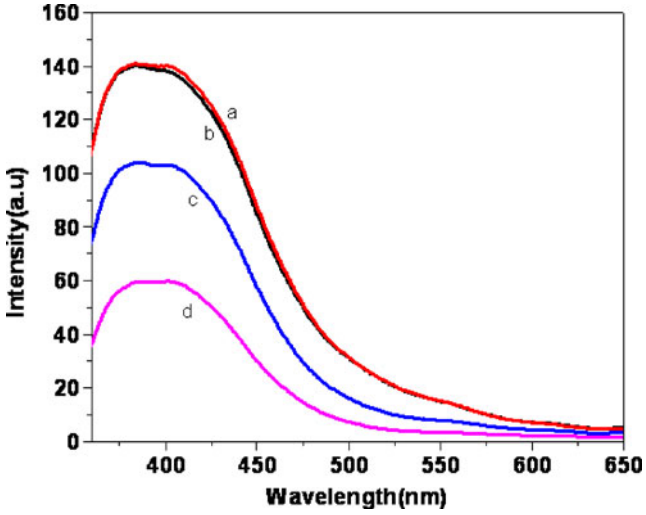

Figure 4. PL spectra of PVK polymer nanoparticles **a.** without Au nanoparticles and in presence of **b.** 3 nm, **c.** 14 nm and **d.** 18 nm Au nanoparticles.

where $K_1 = (K_{sv} + K_s)$ and $K_2 = (K_{sv} \times K_s)$, and K_{sv} and K_s are the dynamic and static quenching constant, respectively. By applying the above equation, static and dynamic quenching constants are being calculated. The obtained values are found imaginary. Therefore, the sphere of action of static quenching model has been introduced to demonstrate the quenching phenomena properly (Thipperudrappa *et al* 2007). According to this model, instantaneous or static quenching occurs if the quencher substances are very near to, or in contact with fluorescent molecules at the moment of its excitation. This is explained by the fact that only a certain fraction, W, of the excited state is actually quenched by the collision mechanism. Some molecules in the excited state, the fraction $(1 - W)$ of which is deactivated almost instantaneously after being formed, because quenchers

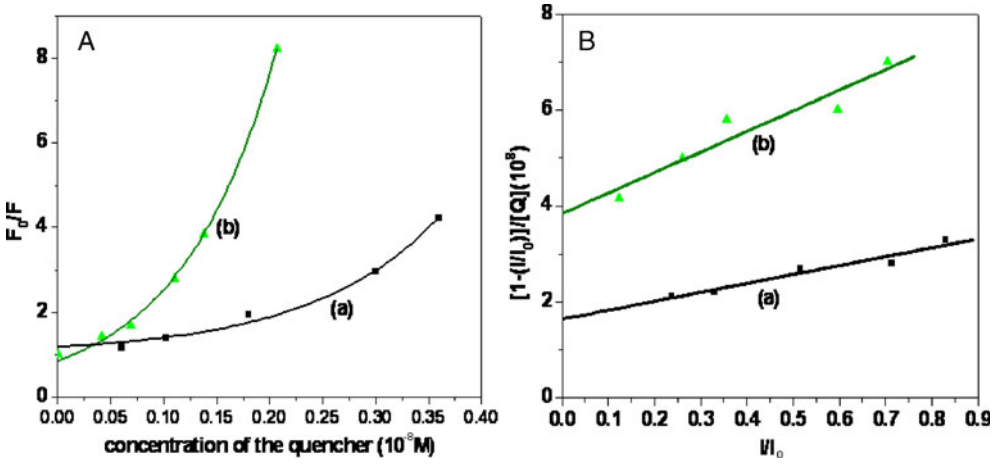

Figure 5. (**A**) Stern–Volmer plot of PVK polymer nanoparticles in presence of **a.** 14 nm and **b.** 18 nm Au nanoparticles and (**B**) $\left[1-(I/I_0)\right]/[Q]$ vs I/I_0 plot of PVK polymer nanoparticles in presence of **a.** 14 nm and **b.** 18 nm Au nanoparticles.

happened to be randomly positioned in the proximity at the time the molecules are being excited. Therefore, we have used the following modified form of S–V equation.

$$(I_0/I) = \{1 + K_{sv}[Q]\}/W. \tag{4}$$

The additional factor, W, is expressed as

$$W = \exp(-V[Q]), \tag{5}$$

where V is the static quenching constant, and it represents an active volume element surrounding in its excited state. Here, W depends on the quencher concentration $[Q]$. At high quencher concentration, the S–V plot deviates from linear character and (4) can be rewritten as

$$\left[1-(I/I_0)\right]/[Q] = K_{sv}(I/I_0) + (1-W)/[Q]. \tag{6}$$

Figure 5b depicts plot of $\left[1-(I/I_0)\right]/[Q]$ against I/I_0 for pure PVK in presence of 14 nm and 18 nm Au nanoparticles as quencher. By calculating the slope and intercept, K_{sv} and V values are calculated. The dynamic and static quenching constants are $1{\cdot}6 \times 10^8$ and $2{\cdot}2 \times 10^8$ M^{-1}, respectively in case of 14 nm Au nanoparticles. The dynamic and static quenching constants are 4×10^8 and $5{\cdot}1 \times 10^8$ M^{-1}, respectively for 18 nm Au nanoparticles. All these data are given in table 1. Both dynamic and static quenching constants increase with increasing size of Au nanoparticles which might increase the probability of dynamic collisions. In our system the dynamic quenching of PVK polymer nanoparticles by quencher Au nanoparticles occurred due to long range electronic energy transfer process. And it mainly depends on the overlap between the absorption spectra of different sized Au nanoparticles and broad emission spectra of PVK polymer nanoparticles. As size of the Au nanoparticles increases, overlap integral also increases, resulting in the increment of dynamic quenching constant. Our results have great consistency with the results described by Cheng *et al* (2006). Besides 'encounter radii' may also

Table 1. PL quenching, static and dynamic quenching constant of PVK nanoparticles in presence of 14 and 18 nm Au nanoparticles.

Systems	PL quenching (%) of PVK nanoparticles (in presence of 0.1×10^{-8} M quencher)	Dynamic quenching constant (M^{-1})	Static quenching constant (M^{-1})
PVK + 14 nm Au	24·2%	$1{\cdot}6 \times 10^8$	$2{\cdot}2 \times 10^8$
PVK + 18 nm Au	57·3%	4×10^8	$5{\cdot}1 \times 10^8$

increase with increase in the quencher nanoparticles size. This may also involve in the increment of dynamic quenching constant. It is very much well known that Au nanoparticle is an efficient quencher for fluorescent dye molecules and semiconducting quantum dots. The dynamic quenching constants are in $\sim 10^6$ M^{-1} order of magnitude in these cases (Huang and Murray 2002; Cheng *et al* 2006). But it should be very high for conjugated polymer systems (Fan *et al* 2003; Bhattacharyya *et al* 2010), because excitonic energy diffusion throughout the polymeric chains plays an important role for energy migration and nonradiative resonance energy transfer towards metal nanoparticles. Fan *et al* (2003) described the superquenching behaviour of cationic fluorescent polymer by Au nanoparticles. The K_{sv} value reached up to $\sim 10^{11}$ M^{-1} in their system. They have also showed that quenching constants increase with increase in quencher Au nanoparticle size. K_{SV} values in our systems are in $\sim 10^8 M^{-1}$ order of magnitude. K_{SV} values are comparatively high for our systems. But it does not reach as high as 10^{11} M^{-1}, because there is neither covalent bonding nor electrostatic interactions between PVK polymer nanoparticles and Au nanoparticles. On the other hand, greater amount of interaction causes greater amount of excited state complexation

(described in sphere of action static quenching mechanism) between PVK polymer nanoparticles and Au nanoparticles. Effective perrin radius for sphere of action may also increase with increase in Au nanoparticle size. Thus, the static quenching constants also increase with increase in size of Au nanoparticles.

3.3 *Time-resolved spectroscopy*

Figure 6 shows decay curves of PVK polymer nanoparticles in absence and presence of different sized Au nanoparticles. In all cases decay curves are fitted by multi-exponential decay. The calculated average decay time of PVK is 0·59 ns. The average decay time of PVK is 0·55 ns in presence of $0{\cdot}1 \times 10^{-8}$ M of 3 nm Au nanoparticles. The average decay times are 0·3 ns and 0·27 ns for PVK nanoparticles in presence of 14 nm and 18 nm Au nanoparticles, respectively. The modification of decay time of PVK in presence of different size of Au nanoparticles is due to both changes in radiative and nonradiative rates. Dulkeith *et al* (2002) showed a shortening of radiative rate and increment of nonradiative rate of lissamine dye in presence of Au nanoparticles. We have also observed the change of radiative and nonradiative rates of PVK polymer nanoparticles in presence of different sized Au nanoparticles. All the values are given in table 2. The observed emission lifetime (τ_{obs}) can be combined with fluorescence quantum yield $\left(\phi_D^0\right)$ to determine the radiative and nonradiative rates separately for all the cases. The following equations are used to determine the radiative and nonradiative rates (Wu *et al* 2000).

$$\kappa_r = \frac{\phi_D^0}{\tau}, \tag{7}$$

$$\kappa_{nr} = \frac{\left(1-\phi_D^0\right)}{\tau}, \tag{8}$$

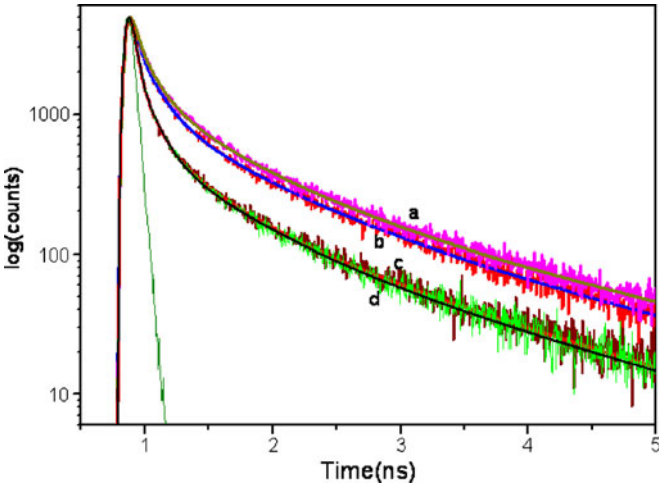

Figure 6. Decay curves of PVK polymer nanoparticles **a.** without Au and in presence of **b.** 3 nm, **c.** 14 nm and **d.** 18 nm Au nanoparticles.

Table 2. Quantum yield, radiative and nonradiative decay rates of PVK nanoparticles in presence of different sized Au nanoparticles.

Systems	Φ_D	Radiative rate (s^{-1})	Nonradiative rate (s^{-1})
PVK	$1{\cdot}13 \times 10^{-2}$	$0{\cdot}19 \times 10^{8}$	$1{\cdot}675 \times 10^{9}$
PVK + 3 nm 'Au'	$1{\cdot}03 \times 10^{-2}$	$0{\cdot}234 \times 10^{8}$	$1{\cdot}77 \times 10^{9}$
PVK + 14 nm 'Au'	$0{\cdot}3 \times 10^{-2}$	$0{\cdot}11 \times 10^{8}$	$3{\cdot}57 \times 10^{9}$
PVK + 18 nm 'Au'	$0{\cdot}07 \times 10^{-2}$	$0{\cdot}025 \times 10^{8}$	$3{\cdot}63 \times 10^{9}$

where κ_r, κ_{nr} are the radiative and nonradiative rate constants, respectively. Quantum yield of each systems have been calculated by using the following equation

$$\phi_D^S = \left(F_s \cdot A_r \cdot n_s^2 \cdot \phi_D^r\right) / \left(F_r \cdot A_s \cdot n_r^2\right),$$

where ϕ_D^S is the quantum yield, F_s and F_r are the integrated fluorescence intensity of the sample and reference, respectively. A_s and A_r are the absorbance at the excitation wavelength of the sample and reference, respectively. ϕ_D^r is the reference quantum yield. From table 2, radiative and nonradiative rates of pure PVK nanoparticles are $0{\cdot}19 \times 10^8$ s^{-1} and $1{\cdot}675 \times 10^9$ s^{-1}, respectively. In presence of 3 nm Au nanoparticles the values are $0{\cdot}234 \times 10^8$ s^{-1} and $1{\cdot}77 \times 10^9$ s^{-1}, respectively. Here, both radiative and nonradiative rates have increased in presence of small Au nanoparticles, whereas the radiative rate decreased and nonradiative rate increased in presence of 14 nm and 18 nm Au nanoparticles. It is very interesting to note that in presence of smaller Au nanoparticles there is increment of radiative rate which suggests that small Au nanoparticles have greater field effect originating from inter-plasmonic interaction. Kim *et al* (2009) described almost the same thing in case of MEH–PPV polymer nanoparticles. The increment of nonradiative rate is also very less in case of 3 nm Au nanoparticles. Therefore, there is no PL-quenching in presence of small 3 nm Au nanoparticles. In presence of 14 nm and 18 nm Au nanoparticles the nonradiative decay rate are notably increasing. The increase of nonradiative decay rate is due to resonance energy transfer which occurs nonradiatively from donor to acceptor. As the size of the quencher nanoparticles increases the nonradiative decay rate increases which confirms greater amount of resonance energy transfer. The energy transfer efficiency can be calculated by using the following equation.

$$\phi_{ET} = 1 - \frac{\tau_{DA}}{\tau_D}, \tag{9}$$

where τ_{DA} and τ_D are the decay time of donor fluorescence in presence and absence of acceptor. By using the above equation the calculated energy transfers are 6·7%, 49·15% and 53·38% for 3 nm, 14 nm and 18 nm Au nanoparticles, respectively. It reveals that energy transfer efficiency varies with size of Au nanoparticles.

Table 3. Energy transfer parameter of PVK polymer nanoparticles in presence of 14 nm and 18 nm Au nanoparticles.

Systems	J (λ) M^{-1} cm^{-1} nm^4	R_0 (Å)	r (Å)	d_0 (Å)	d (Å)	E (%)
PVK + 14 nm 'Au'	$4{\cdot}67 \times 10^{18}$	93·16	91·42	23·5	23·03	52·54
PVK + 18 nm 'Au'	$1{\cdot}56 \times 10^{19}$	113·91	111·91	23·5	22·82	53·38

Again, distance of the donor and acceptor is calculated by using FRET method between PVK and Au nanoparticles. Forster distance R_0 is calculated from the relation

$$R_0 = 0{\cdot}211\left[\kappa^2\eta^{-4}\phi_{\text{donor}}J\,(\lambda)\right]^{1/6}\text{(in angstrom)}\,, \qquad (10)$$

where κ^2 is the orientation factor, ϕ_{donor} the quantum yield of the donor, J (λ) the overlap integral between the absorption spectra of acceptor and emission spectra of the donor. η is the refractive index of the medium. The calculated R_0 values are 93·16 Å and 113·91 Å for 14 nm and 18 nm Au nanoparticles, respectively. The calculated average distances between PVK polymer nanoparticles and Au nanoparticles are 91·42 Å and 111·91 Å, respectively. It is already reported that FRET based method is restricted on the upper limit of only 80 Å. We have calculated the distance between donor and acceptor by using surface energy transfer (SET) method. We calculated d_0 values for each case by using Perrson's model (Chance *et al* 1978; Yan *et al* 2005).

$$d_0 = \left(\frac{0\cdot 255c^3\phi_{\text{D}}^0}{\omega_{\text{d}}^2\omega_{\text{F}}\kappa_{\text{F}}}\right)^{1/4}, \qquad (11)$$

where d_0 is the distance at which a fluorophore will display equal probabilities for energy transfer and spontaneous emission. ϕ_{D}^0 is the quantum efficiency of the fluorophore, ω_{d} the frequency of donor angular electronic transition and ω_{F} and κ_{F} are the angular Fermi frequency and wave vector of the bulk metal. The d_0 value is calculated by using quantum yield of PVK as $1{\cdot}13 \times 10^{-2}$. The calculated ω_{d}^0 value is $4{\cdot}71 \times 10^{15}$ s^{-1}. ω_{F} and κ_{F} are $8{\cdot}4 \times 10^{15}$ s^{-1} and $1{\cdot}2 \times 10^{8}$ s^{-1} and c the velocity of light. The calculated d values are 23·03 Å, 22·82 Å in case of 14 nm and 18 nm Au nanoparticles, respectively. It is already reported that in case of quencher Au nanoparticle SET model is more appropriate due to the various limitations of FRET (Jennings *et al* 2006). Therefore, distance calculated from SET model should be more appropriate in our system. All these values are given in table 3.

4. Conclusions

Here, we showed the Au nanoparticle size dependent study on photoluminescence quenching and energy transfer of PVK polymer nanoparticles. Both static and dynamic quenching constants are increased with increasing size of Au nanoparticles. Radiative and nonradiative rates of PVK have been modified in presence of Au nanoparticles. Analysis suggests that the modification of nonradiative rate indicates the resonance energy transfer between polymer nanoparticles and Au nanoparticles. The percentage of energy transfers are 6·7%, 49·5% and 53·28% for 3 nm, 14 nm and 18 nm Au nanoparticles, respectively. Using surface energy transfer model, the calculated average distances between PVK and Au nanoparticles are 22·03 Å and 23·5 Å for 14 nm and 18 nm Au nanoparticles, respectively. Therefore, photoluminescence quenching, radiative, nonradiative decay and energy transfer efficiency of semiconducting polymer nanoparticles depend on Au nanoparticles size.

Acknowledgements

The CSIR and "Ramanujan Fellowship" are gratefully acknowledged for financial support. One of the authors (SB) thanks CSIR for awarding a fellowship.

References

Bhattacharyya S, Sen T and Patra A 2010 *J. Phys. Chem.* **C114** 11787
Chance R, Prock A and Silbey R 1978 *Adv. Chem. Phys.* **60** 1
Cheng P H, Silvester D, Wang G, Kalyuzhny G, Douglas A and Murrary R W 2006 *J. Phys. Chem.* **B110** 4637
Chowdhury P S, Saha S and Patra A 2005 *Chem. Phys. Lett.* **405** 393
Dulkeith E *et al* 2002 *Phys. Rev. Lett.* **89** 203002
Fan C H, Wang S, Hong J W, Bazan G C, Plaxco K W and Hegger A J 2003 *Proc. Natl. Acad. Sci. U.S.A.* **100** 6297
Frens G 1973 *Nature* **241** 20
Ghosh S K, Pal A, Kundu S, Nath S and Pal T 2004 *Chem. Phys. Lett.* **395** 366
Huang T and Murray R W 2002 *Langmuir* **123** 7077
Jennings T L, Singh M P and Strouse G F 2006 *J. Am. Chem. Soc.* **128** 5462
Kietze T, Nehrer D, Landfester K, Montenegro R, Guntur R and Scherf U 2003 *Natl. Mater.* **2** 408
Kim M S *et al* 2009 *ACS Nano* **3** 1329
Kim S, Lim C K, Na J, Lee Y D, Choi J, Leary J F and Kwon I C 2010 *Chem. Commun.* **46** 1617
Kong F, Sun Y M and Yuan R K 2007 *Nanotechnol.* **18** 265707
Link S and El-Sayed M A 1999 *J. Phys. Chem.* **B103** 8410
Soller T *et al* 2007 *Nano Lett.* **7** 1941
Strouse G F 2005 *J. Am. Chem. Soc.* **127** 3115
Thipperudrappa J, Biradar D S and Hanagodimath S M 2007 *J. Lumin.* **124** 45
Wu F, Zhang J Z, Kho R and Mehra R K 2000 *Chem. Phys. Lett.* **330** 237
Wu C, Bull B, Szymanski C, Christensen K and McNeill J 2008 *ACS Nano* **11** 2415
Yan C S *et al* 2005 *J. Am. Chem. Soc.* **127** 3115
Yu G, Gao J, Hummelen J C, Wudl F and Hegger A J 1995 *Science* **270** 1789